

Biophysical Journal, Volume 115

Supplemental Information

ATP Release by Red Blood Cells under Flow: Model and Simulations

Hengdi Zhang, Zaiyi Shen, Brenna Hogan, Abdul I. Barakat, and Chaouqi Misbah

Supporting Material for ATP Release by Red Blood Cells Under Flow: Model and Simulations

Hengdi Zhang^{1,2}, Zaiyi Shen^{2,3}, Brenna Hogan⁴, Abdul I. Barakat⁴, and Chaouqi Misbah^{1,2*}

¹Univ. Grenoble Alpes, LIPHY, F-38000 Grenoble, France

²CNRS, LIPHY, F-38000 Grenoble, France

³Laboratoire Ondes et Matière d'Aquitaine (LOMA), 351 cours de la libération, 33405 Talence Cedex, France

⁴Laboratoire d'hydrodynamique de l'Ecole polytechnique (LADHYX) 9 Boulevard des Marchaux, 91120 Palaiseau, France

*Correspondence: chaouqi.misbah@univ-grenoble-alpes.fr

Lattice-Boltzmann model for fluid

In the D2Q9 (short for 2 dimensions, 9 discrete velocities) model, the essential variable is the distribution function. A distribution function $f = (f_0, f_1, \dots, f_8)^T$ is defined at a given time step $t_n = n\Delta t$ and on a two dimensional regular mesh $\mathbf{x}_{ij} = (i\Delta x, j\Delta x)$, where i, j and $n \in \mathbf{Z}$, Δt and Δx are the temporal and spatial steps respectively, their ratio $c = \Delta x/\Delta t$ defines the lattice speed. 9 micro-velocities are defined as

$$[\mathbf{c}_0, \mathbf{c}_1 \dots \mathbf{c}_8] = \begin{bmatrix} 0, 1, 0, -1, 0, 1, -1, -1, 1 \\ 0, 0, 1, 0, -1, 1, 1, -1, -1 \end{bmatrix} \cdot c \quad (\text{S1})$$

and macro quantities (density, and thus the pressure, and the velocity field) can be obtained in terms of the micro-velocities and the distribution function

$$[\rho, \rho \mathbf{u}] = \sum_{k=0}^8 [f_k, \mathbf{c}_k f_k] \quad (\text{S2})$$

For the evolution of the distribution function f_k the Bhatnagar-Gross-Krook (BGK) assumption (single relaxation time towards local equilibrium) is adopted and reads

$$f_k(t_{n+1}, \mathbf{x}_{ij} + \mathbf{c}_k \Delta t) = f_k + \frac{1}{\tau_f} (f_k^{eq}(\rho, \mathbf{u}) - f_k) + \Delta t F_k \quad (\text{S3})$$

In which, $\tau_f = 3\mu\Delta t/\rho\Delta x^2 + 1/2$ is the relaxation time, $f_k^{eq}(\rho, \mathbf{u})$ is an equilibrium distribution function defined on the mesh based on macro restrictions,

$$f_k^{eq} = w_k \rho [1 + 3\mathbf{c}_k \cdot \mathbf{u} + 9/2(\mathbf{c}_k \cdot \mathbf{u})^2 - 3/2(\mathbf{u} \cdot \mathbf{u})c^2] \quad (\text{S4})$$

F_k is the body force arising from the vesicle force on the fluid

$$F_k = \left(1 - \frac{1}{2\tau_f}\right) w_k (3(\mathbf{c}_k \cdot \mathbf{u}) + 9(\mathbf{c}_k \cdot \mathbf{u})\mathbf{c}_i) \cdot \mathbf{F} \quad (\text{S5})$$

w_k is the weight factor taking the values $w_0 = 4/9$, $w_{1\sim 4} = 1/9$, $w_{5\sim 8} = 1/36$. It is proven by asymptotic analysis [4] that with condition $\Delta t/\Delta x^2 \sim 1$, Eqn. (S3) converges to Eqn. (3) in the main text with an error term $O(\Delta x^2 + (\mathbf{u}/c)^2)$. From the error term we can infer that the velocity magnitude must be kept small compared to c , typically u/c is taken smaller than 0.005 in this study to ensure a good accuracy. A classic bounce-back treatment [4] is employed to deal with non-slip condition, and we use periodic boundary conditions along the flow direction.

The implementation of periodic and bounce-back boundary conditions is straightforward. However, in the case of a shear flow and a bifurcation in a vessel network, where a velocity has to be imposed at the bounding walls, a special treatment is employed, as described in [5]. The discretization of the vesicle membrane is made via a spring model proposed in [7], which is also well validated in [6]. The vesicle model and fluid equations are coupled via the immersed boundary method (IBM). The crux of the IBM is to replace the 1D membrane as a 2D band having a finite extent (albeit small, typically

of the order of one to two mesh sizes). This is done thanks to a smoothed delta function form in the force term $\mathbf{F}(\mathbf{x})$ from the Navier-Stokes equation Eqn. (3) and the shape evolution equation Eqn. (2) in the main text.

For simulations in shear flow and Poiseuille flow (long straight channel and bifurcation), lattice sizes $\Delta x = 0.15\mu m$ and $0.2\mu m$ are adopted respectively, corresponding to 245 and 183 vertices to represent the vesicle membrane.

Lattice-Boltzmann model for advection-diffusion of the solute

Similar to Navier-Stokes equation, advection-diffusion equations can also be derived from a discrete Boltzmann equation with a proper equilibrium function. The simplest yet effective advection-diffusion lattice boltzmann model is D2Q5 BGK model, which contains 5 discretized micro velocities. We will also use the first five micro velocities defined in Navier-Stokes LBM, see Eqn. (S1). Similar to Navier-Stokes LBM, we start by defining the distribution function g_k on the same mesh as f_k , and the evolution equation of which is given by

$$g_k(t_{n+1}, \mathbf{x}_{ij} + \mathbf{c}_k \Delta t) = g_k + \frac{1}{\tau_g} (g_k^{eq}(\rho, \mathbf{u}) - g_k) + w_k^{(g)} R \quad (\text{S6})$$

The equilibrium distribution function is defined as

$$g_k^{eq} = w_k^{(g)} a (1 + 3\mathbf{c}_k \cdot \mathbf{u}) \quad (\text{S7})$$

The solute concentration can be calculated from g_k from the relation

$$a = \sum_{k=0}^4 g_k, \quad (\text{S8})$$

where $w_0^{(g)} = 1/3$, $w_{1-4}^{(g)} = 1/6$, $\tau_g = 3D\Delta t/\Delta x^2 + 1/2$. Equation (S6) converges to the advection-diffusion Eqn. (5) in the main text with second order precision [4]. The last term on the right hand side $w_k^{(g)} R$ represents the reaction term. As stated before, chemical reactions will not be considered, but we found it worthwhile to mention at this stage how it can easily be implemented.

During time evolution the fictitious particle (whose distribution function g_k is solved outside the vesicle Ω_{ex}) located initially at position \mathbf{x} may collide with a vesicle membrane point represented by \mathbf{X} . The evolution, as seen before, can also be as well represented geometrically by the evolution of the vector \mathbf{x} from \mathbf{x} to $\mathbf{x} + \mathbf{c}_i \Delta t$. At this intersection point we have to specify the boundary condition in a way that mimics the ATP release condition we have adopted. A boundary condition inspired from Bounce-Back in Navier-Stokes LBM is developed to deal with this situation. Marking the right hand side

of Eqn. (S6) as post-collision function g_k^* , the general Neumann boundary condition (Eqn. (6) in the main text) is implemented via replacing Eqn. (S6) by

$$g_{\bar{k}}(t_{n+1}) = \frac{c + 3(\mathbf{u} \cdot \mathbf{c}_k)}{c - 3(\mathbf{u} \cdot \mathbf{c}_k)} g_k^* + \frac{1}{c - 3(\mathbf{u} \cdot \mathbf{c}_k)} D \cdot \psi \quad (\text{S9})$$

Recall that ψ is the ATP release condition that depends on local states of the membrane. The subscript \bar{k} represents the direction that opposite to direction of g_k . This boundary condition provides second order precision if the boundary is parallel to the mesh of the lattice, otherwise it has first order precision (for a curved boundary or a straight boundary which is tilted with respect to the lattice)[3]. It is worth mentioning that for a static boundary and zero-flux condition, where \mathbf{u} and F are both zero, the boundary scheme Eqn. (S9) will reduce to a pure bounce-back scheme.

The concentration a is defined only in Ω_{ex} . In situations when the vesicle shape evolves, a lattice point located near $\mathbf{X}(s)$ may lie in Ω_{in} at a given time step but flip into Ω_{ex} in the new time step. A refilling process is needed. The evolution equation of the distribution function g_k is composed of a linear advection term, represented by \mathbf{c}_k , and a non-linear BGK collision term. This mixture of terms makes the numerical scheme a formidable task. A second order extrapolation scheme is implemented here as a result of compromise between accuracy and computational complexity.

As shown in Fig. S1, let us assume that a cell tumbling motion causes a lattice to flip from Ω_{in} into Ω_{ex} . A set of neighboring points is required for a lattice refilling process. A collection of subscripts $S = \{k | k \in [1, 2 \dots 4], \mathbf{x} + \mathbf{c}_k \in \Omega_{ex}, \mathbf{x} + 2\mathbf{c}_k \in \Omega_{ex}\}$ is defined on the lattice \mathbf{x} . The refill process can be written as

$$g_k = \frac{\sum_{k' \in S_{refill}} w_{k'} [2g_k(t, \mathbf{x} + \mathbf{c}_{k'}) - g_k(t, \mathbf{x} + 2\mathbf{c}_{k'})]}{\sum_{k' \in S_{refill}} w_{k'}} \quad (\text{S10})$$

This refill process introduces an acceptable cumulative error in the simulations time scales of interest. Note that the maximum velocity for vesicle must be significantly smaller than c , which is already satisfied in the IBM coupled LBM solver.

In all simulations, the ATP concentration is solved on the same mesh as that used for the fluid.

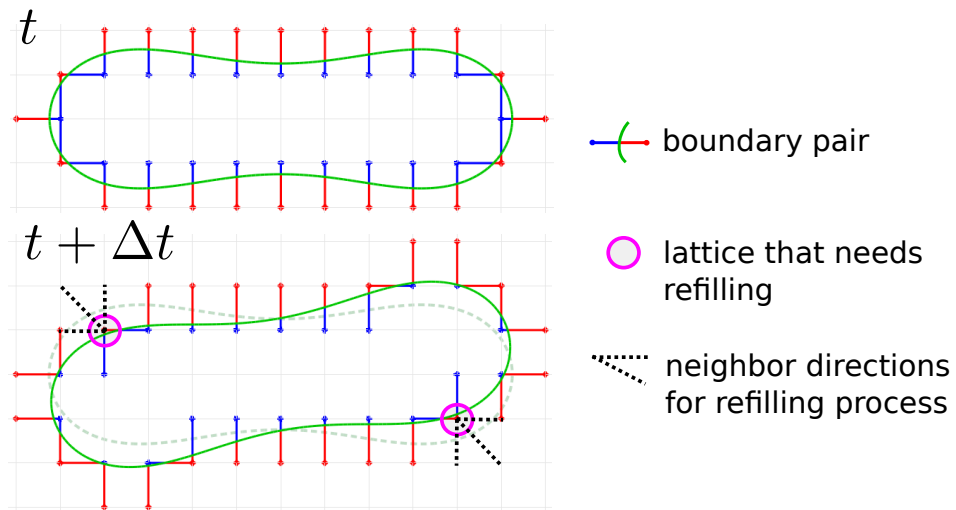


Figure S1: Schematics for refill process of boundary lattices

Mean membrane / apparent shear stress in shear simulation

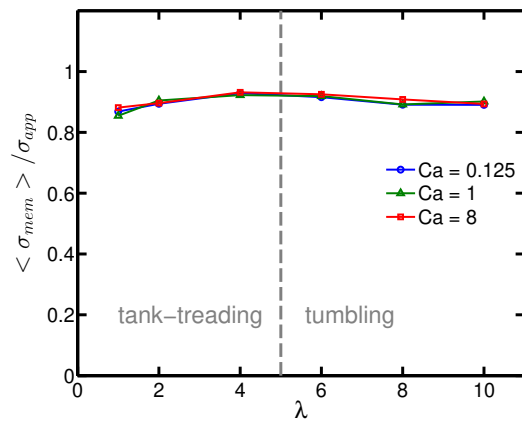


Figure S2: Shear stress vs viscosity contrast

ATP release level under shear with different μ_{in} and fixed $\mu_{ex} = 1 \text{ mPa}\cdot\text{s}$

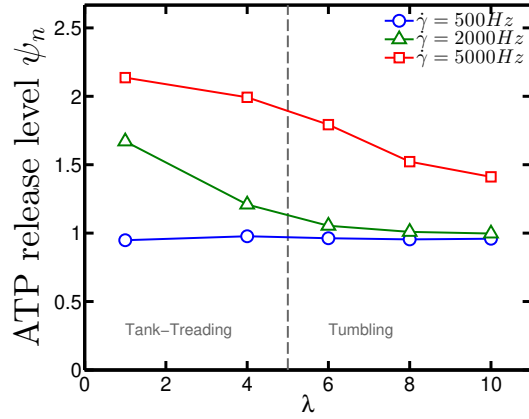


Figure S3: Under linear shear flow with an adequately large shear rate, increasing μ_{in} (as well as $\lambda = \mu_{in}/\mu_{ex}$) results in a drop of ATP release level due to the reduction of curvature change in TT to TB transition.

Mean shear stress and deformation level in a long straight channel

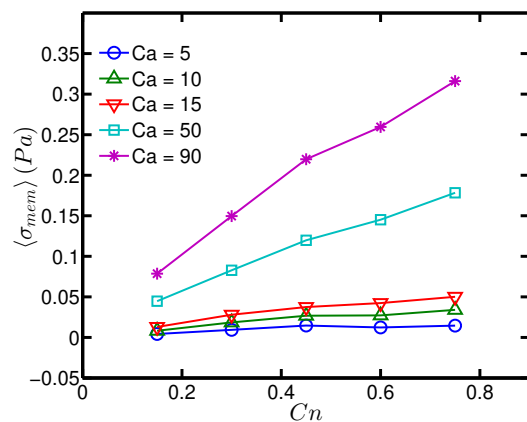


Figure S4: mean shear stress in long straight channel

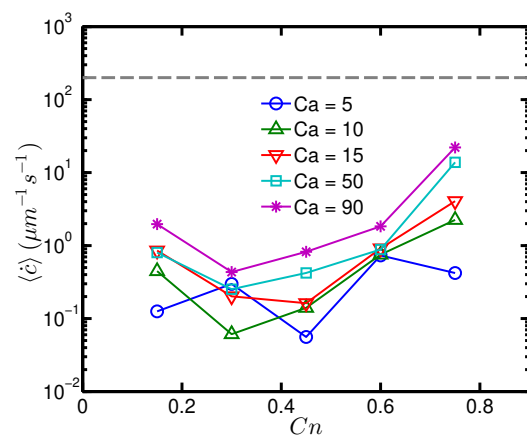


Figure S5: mean curvature change in long straight channel

Since the gray dashed line in Fig. S5 represents the critical curvature change $\dot{c}_c = 200 \mu\text{m}^{-1}\text{s}^{-1}$, it is clearly seen that the ATP release levels in long straight channel are not affected by shape deformation, but only by shear stress.

Estimation of the phenomenological ATP flux coefficient k_σ

From the experimental configuration in [1] we know that the RBC solution has a Hematocrit $h_t = 1\%$. The suspension is subjected to a linear shear flow for a period of time $T = 30$ s. Comparing to typical plasma ATP concentration $a_0 = 1000$ nmol/L (value from [2]), the experiments [1] reported that the relative amount (compared to static conditions) of ATP release is three-fold, $f = 3$, in the plateau regime of Fig. 2 (upper) in the main text. The total amount of ATP release from a RBC during this 30 s can then be estimated as

$$\Phi_{tot} = f a_0 \cdot \left(\frac{4}{3}\pi R_0^3 \tau / h_t\right) \quad (\text{S11})$$

Since our ATP release criterion is based on the surface stress of the cell, k_σ has a dimension of a flux per unit area and unit time, and taking $4\pi R_0^2$ for the area of a RBC, we obtain the following estimate for k_σ

$$\begin{aligned} k_\sigma &\approx \frac{\Phi_{tot}}{4\pi R_0^2 \cdot T} \\ &\approx 7 \times 10^3 (\text{nmol/L}) \cdot \mu\text{m/s} \end{aligned} \quad (\text{S12})$$

Recall that the characteristic radius $R_0 = 3\mu\text{m}$ and the reduced volume (or reduced area in 2D) $\tau = 0.7$.

Lateral migration of a RBC after bifurcation

We have investigate different angles (defined in Fig. S6) between feeding channel and down-stream branching channels. The angles are varied in the range of $0^\circ < \theta_1, \theta_2 < 90^\circ$ with an indentation of 30° . Moreover, we have initially set the vesicle at different positions, such are: center-line (lateral position 0), faster zone (lateral position 0.25) and slower zone (lateral position -0.25); see Fig. S6. The capillary numbers are taken as $Ca = 5$ and 50 (as defined in the main article, Ca is proportional to velocity). The confinement $Cn = 0.3$ is chosen to be the same value as used in the main text.

We find for most cases that when a vesicle is initially located at the center-line it will be "scattered" to an off-centered lateral position (the middle panel in Fig. S6 (b)). Consider a vesicle in a vessel network, which has been off-centered. After some time it has some probability to go back to the center-line if it enters the faster zone of a daughter branch (the upper panel in Fig. S6 (b)). However, even if it goes back to the centerline by this scenario, this vesicle will be again scattered towards off-centered position after the next bifurcation. When a vesicle enter the slower zone, its probability to get off-centered becomes high (see the lower panel in Fig. S6).

This gives a hint to the idea that within a complex vessel network (with many bifurcations), an RBC will often go to off-center position due to the presence of bifurcations.

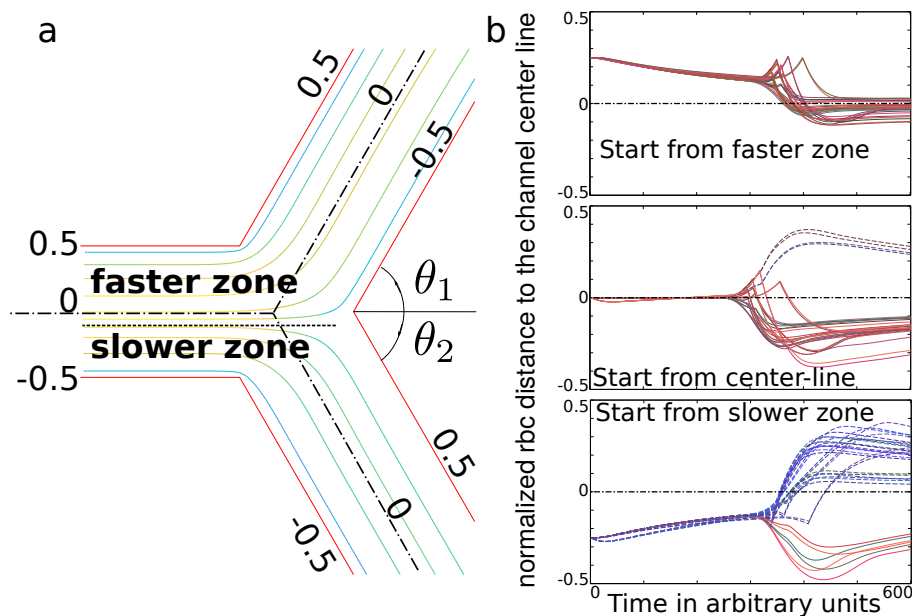


Figure S6: (a) Schematic for definition of θ_1, θ_2 , normalized lateral position and faster (upper) / slower (lower) zone. The dashed line represents the border (or separation line) for streamlines entering faster or slower branch. Streamlines are solid lines with colors representing their relative velocity (yellow for fast, green for median and blue for slow). The dashed-dotted lines represent the centerlines of feeding and branching channels. A normalized lateral distance of two parallel walls in a given channel is defined as -0.5 and 0.5 , counted from the centerline (the latter is defined to be the zero line). (b) Simulation results with different bifurcation angles, initial position and speeds. Curves on the right panel rendered in red indicate that the RBCs enter the faster branch, while colors close to blue refer to RBCs entering the slower branch.

SUPPORTING REFERENCES

- [1] Alison M. Forsyth, Jiandi Wan, Philip D. Owrutsky, Manouk Abkarian, and Howard A. Stone. Multiscale approach to link red blood cell dynamics, shear viscosity, and atp release. *Proc. Natl. Acad. Sci. USA.*, 108(27):10986–10991, 2011.
- [2] Mark W Gorman, Eric O Feigl, and Charles W Buffington. Human

- plasma atp concentration. *Clin. Chem.*, 53(2):318–325, 2007.
- [3] Juntao Huang and Wen-An Yong. Boundary conditions of the lattice boltzmann method for convection–diffusion equations. *J. Comput. Phys.*, 300:70–91, 2015.
 - [4] Timm Krüger, Halim Kusumaatmaja, Alexandr Kuzmin, Orest Shardt, Goncalo Silva, and Erlend Magnus Viggen. *The Lattice Boltzmann Method*. Springer, 2017.
 - [5] A. J. C. Ladd and R. Verberg. Lattice-boltzmann simulations of particle-fluid suspensions. *Journal of Statistical Physics*, 104(5):1191–1251, Sep 2001.
 - [6] Zaiyi Shen, Alexander Farutin, Marine Thiébaud, and Chaouqi Misbah. Interaction and rheology of vesicle suspensions in confined shear flow. *Phys. Rev. Fluids*, 2:103101, Oct 2017.
 - [7] Ken-ichi Tsubota and Shigeo Wada. Effect of the natural state of an elastic cellular membrane on tank-treading and tumbling motions of a single red blood cell. *Phys. Rev. E*, 81(1):011910, 2010.